

## Neogene climate change and emergence of C<sub>4</sub> grasses in the Namib, southwestern Africa, as reflected in ratite <sup>13</sup>C and <sup>18</sup>O

Loïc Ségalen<sup>a,b,\*</sup>, Maurice Renard<sup>a</sup>, Julia A. Lee-Thorp<sup>b,c</sup>, Laurent Emmanuel<sup>a</sup>,  
Laurence Le Callonnec<sup>a</sup>, Marc de Rafélis<sup>a</sup>, Brigitte Senut<sup>d</sup>,  
Martin Pickford<sup>d,e</sup>, Jean-Luc Melice<sup>f</sup>

<sup>a</sup> Laboratoire de Biominéralisations et Paléoenvironnements, Université Pierre et Marie Curie, JE 2477, case 116, 4 place Jussieu, 75252 Paris cedex 05, France

<sup>b</sup> Quaternary Research Centre and Department of Archaeology, University of Cape Town, Private Bag, Rondebosch 7701, South Africa

<sup>c</sup> Department of Archaeological Sciences, University of Bradford, Bradford BD7 1DP, United Kingdom

<sup>d</sup> Département “Histoire de la Terre”, Muséum National d’Histoire Naturelle, USM 203 et UMR 5143 CNRS, case 38, 57 rue Cuvier, 75231 Paris cedex 05, France

<sup>e</sup> Chaire de Paléanthropologie et de Préhistoire, Collège de France, UMR 5143 CNRS, 11 place Marcellin Berthelot, 75005 Paris, France

<sup>f</sup> Institut de Recherche pour le Développement, Department of Oceanography, University of Cape Town, Private Bag, Rondebosch 7701, South Africa

Received 23 June 2005; received in revised form 11 December 2005; accepted 16 December 2005

Available online 29 March 2006

Editor: E. Boyle

### Abstract

Stable light isotopes in ratite eggshells have been shown to be reliable indicators of shifts in climate and environmental conditions in the past. Here, we show that  $\delta^{18}\text{O}$  and  $\delta^{13}\text{C}$  values in fossil and modern ratite eggshells collected in the aeolianite deposits of the southern and central Namib Desert track regional distinctions and global climate shifts throughout the Neogene.  $\delta^{18}\text{O}$  values, although variable, are consistently higher in the central compared to the southern Namib throughout the record.  $\delta^{18}\text{O}$  trends during the Miocene differ for the two regions, but track each other post-Miocene. Throughout the Miocene,  $\delta^{13}\text{C}$  values for ratite eggshells from both the central and southern Namib regions are indistinguishable showing that the flora remained C<sub>3</sub> throughout. The overall negative (–3%) shift in mean values for Miocene biostratigraphic zones is consistent with the response of C<sub>3</sub> photosynthesis to  $p\text{CO}_2$  shifts from 180 to 320 ppmv as estimated from marine alkenone studies and/or evolution of the  $\delta^{13}\text{C}$  of the atmospheric CO<sub>2</sub>. Evidence for C<sub>4</sub> plants occurs post-Miocene, with the development of the southern, winter rainfall and central/northern, summer rainfall zonation apparent today. These data provide independent corroboration that the expansion of C<sub>4</sub>-dominated ecosystems after ~7 Ma cannot be attributed to a reduction of  $p\text{CO}_2$  below a 500 ppmv threshold, as earlier proposed. Proliferation of C<sub>4</sub> plants in the Namib after ~5 Ma and, elsewhere, may be related rather to energy budgets and rainfall seasonality shifts resulting from large-scale atmospheric and oceanic circulation reorganisation.

© 2005 Elsevier B.V. All rights reserved.

**Keywords:** Miocene; ratite eggshells; Namib Desert; stable isotopes;  $p\text{CO}_2$ ; C<sub>4</sub> expansion

\* Corresponding author. Laboratoire de Biominéralisations et Paléoenvironnements, Université Pierre et Marie Curie, JE 2477, case 116, 4 place Jussieu, 75252 Paris cedex 05, France.

E-mail address: [segalen@ccr.jussieu.fr](mailto:segalen@ccr.jussieu.fr) (L. Ségalen).

## 1. Introduction

The Neogene is characterized by the transition of a warm climate to an “icehouse world” during the Miocene, in which a series of events modified global climate with long-lasting impacts on continental system biota and the climatic zones.

One factor that has been held to be an important driver is the concentration of the greenhouse gas CO<sub>2</sub>; indeed long-term shifts in *p*CO<sub>2</sub> are of considerable interest for assessing responses of the earth’s climate. The large-scale radiation of C<sub>4</sub> plants in low and mid-latitudes in the Late Miocene, documented by shifts in carbon isotope values of soil carbonates and faunal enamel [1–4], has been attributed to an abrupt lowering of *p*CO<sub>2</sub> levels to below 500 ppmv [4], based partly on a reading of Berner’s ocean/atmosphere equilibrium model [5] and partly on the known efficiency of C<sub>4</sub> plants in capturing CO<sub>2</sub> under low *p*CO<sub>2</sub> conditions [6].

Although it is generally understood that atmospheric *p*CO<sub>2</sub> has diminished markedly since the Eocene, no direct measures of *p*CO<sub>2</sub> are available beyond ice-core data to 740 ky [7]. Most estimates of secular *p*CO<sub>2</sub> changes rely on models invoking equilibria between the ocean and atmosphere that require approximations of pH and proxy data from marine sediment cores. More recently, a detailed sequence of *p*CO<sub>2</sub> from 25 to 5 My was constructed from diunsaturated alkenone δ<sup>13</sup>C data from an oligotrophic Pacific Deep Sea Drilling Project core, which suggested that *p*CO<sub>2</sub> varied from ca. 180–220 ppmv at 14–16 My to ca. 260–320 ppmv at 5–9 My [8,9]. Sparser data from an independent study that refined surface ocean pH deduced from boron isotope ratios of planktonic foraminifera also suggested low *p*CO<sub>2</sub> throughout the Neogene [10]. Hence, both studies suggest that low *p*CO<sub>2</sub> existed throughout the Miocene, based on marine proxy data. If confirmed, the mechanism(s) promoting spread of C<sub>4</sub> in the Upper Miocene must be carefully re-examined.

To date, most studies detailing the emergence of substantial C<sub>4</sub> components in African ecosystems have been based in East Africa. The exceptions are a study of ~5 My Langebaanweg material that demonstrated absence of C<sub>4</sub> plants at the southwestern tip of Africa [11], and ongoing work in Chad where only the Pliocene data have been published so far [12]. Based on studies in other parts of the world, Cerling et al. have argued that C<sub>4</sub> grasses first appeared as significant components of the vegetation in the tropics, and subsequently spread to mid-latitudes [4]. In this study, we examine shifts in floral composition from the perspective of a western low- to mid-latitude region of Africa, in concert with

climate and ocean circulation shifts, using carbon and oxygen isotope ratios in a sequence of fossil ratite eggshells. Elsewhere, stable isotope data from Late Pleistocene and Holocene African ostrich eggshells [13–15] and from Miocene ratite eggshells [16] have been used to track floral and climate shifts in southern Africa and Pakistan, respectively. We use the results to test the proposal for sequential C<sub>4</sub> appearance from low latitudes outwards for Africa, and to establish patterns of floral and climate changes across a broader region, which can in turn help us to discern the drivers of these major shifts in the Upper Miocene and more recent eras.

## 2. Stable light isotopes in the continental biosphere

### 2.1. <sup>13</sup>C/<sup>12</sup>C ratios

Plant carbon isotopic signatures reflect discrimination against <sup>13</sup>C in photosynthesis [17–19] including isotope effects during diffusion of atmospheric CO<sub>2</sub> into the intercellular leaf spaces, and enzymatic activity of RuBP carboxylase (C<sub>3</sub>, C<sub>4</sub> plants and CAM pathways during the diurnal phase) and/or phosphoenolpyruvate carboxylase (C<sub>4</sub> plants and CAM pathways during the nocturnal phase). The δ<sup>13</sup>C values of C<sub>3</sub> and C<sub>4</sub> plants are distinct, with means of –27‰ (range –35‰ to –21‰) and –13‰ (range –15‰ to –10‰), respectively. CAM plants may have intermediate values from –10‰ to –22‰ depending on conditions and whether or not they are obligate CAM. C<sub>4</sub> plants effectively concentrate CO<sub>2</sub> as an initial step, but in C<sub>3</sub> plants fractionation is influenced by the ratio of CO<sub>2</sub> concentration in the intercellular space (*c<sub>i</sub>*) to CO<sub>2</sub> concentration in the atmosphere (*c<sub>a</sub>*) [17–19]. During CO<sub>2</sub> uptake stomata remain open, exposing plants to water loss. Hence, δ<sup>13</sup>C in C<sub>3</sub> plants is sensitive to variations in atmospheric *p*CO<sub>2</sub> (fractionation of –0.02‰/ppmv; [20]) and to aridity [21]. C<sub>4</sub> plants can tolerate arid conditions, although primarily high radiation and warm temperatures in the growing season control distribution of C<sub>4</sub> grasses [6].

### 2.2. <sup>18</sup>O/<sup>16</sup>O ratios

Oxygen isotope ratios in rainwater (δ<sup>18</sup>O<sub>mw</sub>) are a function of condensation temperature – implicating latitude, altitude and seasonal temperature fluctuations – as well as Rayleigh distillation effects and volume of precipitation [22]. In arid areas such as the Namib, evaporation due to low relative humidity and high soil temperatures promotes enrichment in <sup>18</sup>O in environmental water. Soil water taken up by plants may be

further enriched in  $^{18}\text{O}$  in leaves as a result of evapo-transpiration effects. Thus,  $\delta^{18}\text{O}$  of both leaf water and carbohydrates in leaves are significantly enriched in  $^{18}\text{O}$  by up to 15‰ [23–25] under conditions of low relative humidity (i.e. warm, dry conditions).

### 3. Namib Desert isotopic ecology and modern eggshells

In the Namib, two different ecosystems currently prevail, controlled by the timing of the meagre rainy seasons (Fig. 1). The South Atlantic High Pressure (SAHP) system moves southwest during the austral summer, allowing occasional penetration of moisture-bearing easterlies to the central and northern Namib, and northeast in winter, exposing the southern Namib to the influence of expanded circumpolar westerlies, and therefore at the westerlies rainfall system. The wind-driven Benguela coastal upwelling system is directly related to the position and strength of the SAHP gyre. Plant cover south of Lüderitz in the winter rain belt consists of  $\text{C}_3$  and

succulent (CAM) plants, while  $\text{C}_4$  grasses occur in the central and northern Namib Desert where rain occurs in summer (Fig. 1) related to the tropical rainfall system.

In our study, we used  $\delta^{13}\text{C}$  and  $\delta^{18}\text{O}$  in eggshells as a reflection of diet and climate conditions. The results reflect conditions experienced by ostriches during the reproductive season, which is timed to coincide with onset of the rainy season [26]. The African ostrich (*Struthio camelus*) is a mixed feeder well adapted to arid conditions. They are non-obligate drinkers that obtain most of their water requirements from leaf-water. Therefore, eggshell  $\delta^{18}\text{O}$  largely reflects the influence of relative humidity (comprising elements of moisture availability and air temperatures) on plants in addition to other considerations related to average  $\delta^{18}\text{O}_{\text{mw}}$  values [14,15]. Ostriches prefer tender green annual grasses and forbs, and when not available, leaves, flowers and fruits of succulents and woody plants [27]. Thus, in the central and northern Namib, their diets consist of  $\text{C}_3$ ,  $\text{C}_4$  and CAM plants, and in the south,  $\text{C}_3$  and CAM plants. Eggshell carbonate is enriched by  $\sim 15\text{--}16\text{‰}$  in  $^{13}\text{C}$  relative to the ingested food [14,26].

Mean  $\delta^{13}\text{C}$  values for modern ostrich eggshell from the southern and central Namib regions are distinct, at  $-6.10 \pm 1.90\text{‰}$  and  $-3.65 \pm 2.40\text{‰}$ , respectively ( $t$ -test,  $t=3.135$ ,  $df=30$ ,  $p=0.004$ , Appendix B.3). These data are in accordance with plant distributions in the two regions, despite variability due to fluctuations in conditions during the reproductive season. Mean  $\delta^{18}\text{O}$  for modern ostrich eggshells from the two regions are also significantly different, at  $9.55 \pm 2.70\text{‰}$  in the southern and  $14.20 \pm 2.15\text{‰}$  in the central Namib, respectively ( $t$ -test,  $t=4.923$ ,  $df=30$ ,  $p<0.001$ , Appendix B.3) ( $\delta^{18}\text{O}$  is expressed vs. PDB). These high values confirm the influence of enriched plant water, due to evapo-transpiration effects, on ostrich body water and eggshell  $\delta^{18}\text{O}$  values. It seems reasonable, therefore, that similar isotope effects hold for the eggshells of fossil ratites since they too inhabited largely arid areas.

## 4. Materials and methods

### 4.1. Diagenetic aspects

Prior to isotopic analysis of fossil ratite eggshells, we checked their state of preservation using cathodoluminescence with a Technosyn 8200 Mk II luminoscope at 15 kV and 350–400 mA, and X-ray diffraction. Eggshells are composed of low-magnesium calcite. Under cathodoluminescence, modern and fossil ratite eggshells show a non-luminescent (dark bluish to dark brown) calcite, interpreted as primary, based on results

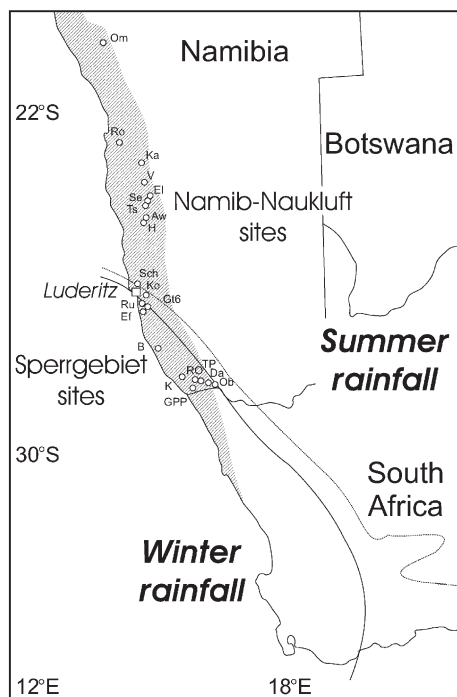


Fig. 1. The west coast of southern Africa showing the Namib Desert (hatching) and areas where modern and fossil eggshells were collected, and the seasonal rainfall geographic limits. (AW: Awasib, B: Buntfeldschuh, Da: Daberas, Ef: Elisabethfeld, El: Elim, H: Haiber, GPP: Gypsum Plate Pan, GT6: Grillental 6, K: Karingarab, Ka: Kamberg, Ko: Kolmanskop, La: Langental, Ob: Obib, Om: Omaruru, RO: Rooilepel, Ro: Rooibank, Ru: Russel's Perch, Sch: Schmitfeld, Se: Sesriem, TP: Target Pan, Ts: Tsauchab, V: Vreemdelingspoort).

from modern biogenic calcite [28,29].  $Mn^{2+}$  is the main activator for luminescence phenomena in calcite. Concentrations of  $Mn^{2+}$  are very low for modern specimens, between 2.03 ppm and 0.11 ppm (mean value 1.24,  $n=12$ ), and remain low, between 9.7 ppm and 0.12 ppm (mean value 1.12 ppm,  $n=70$ ) for the fossils [30]. Therefore, concentrations remain below 10 ppm, the critical value necessary to observe the luminescence in optical microscopy [31]. The exceptions are observations of bright orange luminescence in the pore complexes where secondary calcite with higher concentrations of the  $Mn^{2+}$  activator has formed. These regions contrast strongly with the dark bluish colour observed for the rest of the shell.

#### 4.2. Sample preparation

To offset the effects of secondary carbonate deposition, which is observed in the pore structures, the external and internal surfaces of the eggshells were cleaned by abrasion and ultrasound, and the samples (total ~260) were extracted from the thickest (non-eroded) parts of the shell and far from pore complexes (many of which showed secondary  $CaCO_3$  deposition). Isotopic analysis was performed using two methods. In

the first, 10 mg of biogenic carbonate was reacted with  $H_3PO_4$  acid at 25 °C for 12 h, and  $^{13}C/^{12}C$  and  $^{18}O/^{16}O$  ratios measured on a SIRA9/VG602 spectrometer (University PARIS 6). For the second method, applicable to fewer samples, 0.08 mg of biogenic carbonate was analysed for  $^{13}C/^{12}C$  and  $^{18}O/^{16}O$  ratios using a Kiel II autocarbonate device (whereby each sample is reacted with 100% phosphoric acid at 70 °C) coupled to a Finnigan MAT 252 mass spectrometer (University of Cape Town).  $\delta^{13}C$  and  $\delta^{18}O$  by convention is reported in the  $\delta$  notation relative to the international standard PDB, in parts per mil, as:  $\delta^{13}C$  (‰) =  $[(^{13}C/^{12}C)_{sample}/(^{13}C/^{12}C)_{std} - 1] * 1000$  and  $\delta^{18}O$  (‰) =  $[(^{18}O/^{16}O)_{sample}/(^{18}O/^{16}O)_{std} - 1] * 1000$ . Analytical precision for  $\delta^{13}C$  and  $\delta^{18}O$  is 0.1‰ for both methods.

## 5. Results

### 5.1. $\delta^{13}C$ trends

We constructed a terrestrial chronostratigraphic sequence of ratite eggshells (Fig. 2) collected from aeolianites at central and southern Namib outcrops (Fig. 1) that represents a series of discrete biostratigraphic zones through the last 20 Ma (Appendices A and B.1, B.2, B.3,

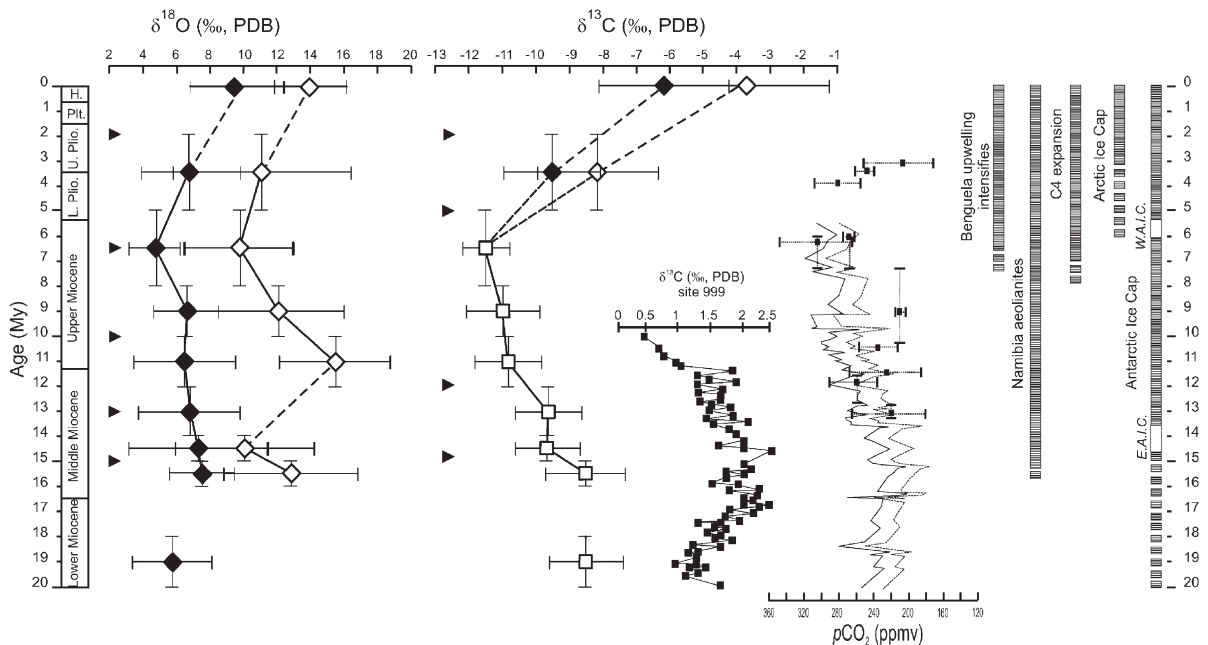


Fig. 2. Trends in  $\delta^{18}O$ ,  $\delta^{13}C$  of Namib ratite eggshells during the Neogene. Comparison with  $pCO_2$  (ppmv) as calculated from Pagan et al. [8,9] (range shown as two solid lines) and Pearson and Palmer [10] (■ with error bars), the  $\delta^{13}C$  carbonate record from site 999 [34], and major global and regional climatic events. After the Late Miocene,  $\delta^{13}C$  in eggshells of the southern (◆) and the central Namib (◇) is statistically distinct.  $\delta^{18}O$  trend is distinct throughout the Neogene between the southern and the central Namib. Abbreviations: EAIC = East Antarctic Ice Cap, WAIC = West Antarctic Ice Cap, ► = shifts statistically significant (see Appendix B). All the data are available in supplementary information (Table 1 in the Appendix).

and B.4, [30,32]). Throughout the Miocene, eggshell  $\delta^{13}\text{C}$  indicates that ostrich diets were predominantly to exclusively  $\text{C}_3$  (Fig. 2) and that the central and southern Namib data are indistinguishable ( $t$ -test,  $p > 0.05$ , Appendix B.3). The oldest eggshells (Aepyornithoid type, Early Miocene: 18–20 Ma) are associated with fluvial deposits and the highest mean  $\delta^{13}\text{C}$  value for the Lower Miocene of  $-8.45 \pm 1\text{‰}$  (Fig. 2, Appendix B.1). Two significant negative shifts to  $-9.65 \pm 0.95\text{‰}$  ( $t$ -test,  $t = 4.312$ ,  $df = 50$ ,  $p < 0.001$ , Appendix B.4) and  $-10.75 \pm 0.95\text{‰}$  ( $t$ -test,  $t = 4.348$ ,  $df = 72$ ,  $p < 0.001$ , Appendix B.4), respectively, occurred in the Middle Miocene, followed by further shifts reaching  $-11.50 \pm 0.70\text{‰}$  during the latest Miocene (Fig. 2). Data from the single biostratigraphic zone in the Pliocene and from modern eggshells show that ratite eggshell  $\delta^{13}\text{C}$  values from the central and southern Namib diverged at some point after the latest Miocene ( $t$ -test,  $p < 0.05$ , Appendix B.3) (Fig. 2).  $\delta^{13}\text{C}$  increases significantly in both regions ( $t$ -test,  $p < 0.001$ , Appendix B.4), but more strongly in the central Namib, showing means of, respectively,  $-9.50 \pm 1.45\text{‰}$  and  $-8.20 \pm 1.45\text{‰}$  during the Pliocene and also for the modern eggshells as indicated above.

## 5.2. $\delta^{18}\text{O}$ trends

Despite a high  $\delta^{18}\text{O}$  range for each biostratigraphic layer (showing standard deviations of 1.10‰ to 4.15‰), the data show two trends between the southern and central Namib, with an offset between the southern and the central Namib of 2.5 to 9 per mil (Fig. 2).

In the southern Namib,  $\delta^{18}\text{O}$  values for each biostratigraphic zone are consistently between 5.85‰ and 7.35‰ during the Early Miocene to the Upper Miocene. These variations between  $^{18}\text{O}$  are not significant ( $t$ -test,  $p > 0.05$ , Appendix B.5). Following a slight decrease to  $4.70 \pm 1.45\text{‰}$  at the latest Miocene (not significant compared to previous layer,  $t$ -test,  $p > 0.05$ , Appendix B.5),  $\delta^{18}\text{O}$  increases to  $6.70 \pm 2.80\text{‰}$  during the Pliocene and again to  $9.55 \pm 2.70\text{‰}$  for the modern specimens (Fig. 2); this last shift from Pliocene to modern is statistically different ( $t$ -test,  $t = 2.744$ ,  $df = 29$ ,  $p = 0.010$ , Appendix B.5).  $\delta^{18}\text{O}$  values obtained during the Mio-Pliocene are similar to the  $^{18}\text{O}$  ranges observed for modern eggshells at Elands Bay further south on the west coast of South Africa ( $\sim 6\text{‰}$ , [15]). Hence, these values likely reflect somewhat moister/cooler conditions in the southern Namib during this period, although Elands Bay conditions are still classed as arid, with mean annual rainfall  $< 350$  mm [15].

In the central Namib, the  $\delta^{18}\text{O}$  of ratite eggshells is significantly higher ( $t$ -test,  $p < 0.05$ , Appendix B.3), with the exception of one biozone (see below). The record shows large fluctuations between  $10.05 \pm 4.10\text{‰}$  and  $15.45 \pm 3.25\text{‰}$  during the Middle to Upper Miocene (Fig. 2 and Appendix B.2). During the Middle Miocene,  $\delta^{18}\text{O}$  decreases from  $12.80 \pm 4\text{‰}$  to  $10.05 \pm 4.10\text{‰}$ , with an offset of only  $\sim 2.5\text{‰}$  compared to southern Namib values (Fig. 2). At this period only, the difference between the two areas is not significant ( $t$ -test,  $t = 1.779$ ,  $df = 28$ ,  $p = 0.087$ ). Thereafter, a significant shift to a higher mean  $\delta^{18}\text{O}$  of  $15.45 \pm 3.25\text{‰}$  occurs during the Upper Miocene ( $t$ -test,  $t = 4.234$ ,  $df = 33$ ,  $p < 0.001$ , Appendix B.6), with large offsets of  $\sim 9\text{‰}$  compared to the southern Namib mean (Fig. 2). The shift to  $9.75 \pm 3.25\text{‰}$  in the latest Miocene is significant ( $t$ -test,  $t = 4.574$ ,  $df = 26$ ,  $p < 0.001$ , Appendix B.6), implying slightly moister or cooler conditions in the central Namib (that is, compared to earlier high values implying extreme aridity). Shifts to higher values occur thereafter, from Pliocene  $\delta^{18}\text{O}$  of  $10.45 \pm 5.50\text{‰}$  to modern mean of  $14.20 \pm 2.15\text{‰}$ . Of these shifts, only the difference between latest Miocene and modern eggshell values is significant ( $t$ -test,  $t = 3.831$ ,  $df = 21$ ,  $p = 0.001$ , Appendix B.5).

Despite the offset, and earlier Miocene differences between the two trends reflecting two sets of climatic conditions in the southern and central Namib, both records indicate near-continuous aridity, with the exception of lower means at the latest Miocene that may be related to a diminution of aridity or cooler conditions in the Namib. From the Pliocene to the Present,  $\delta^{18}\text{O}$  increases in both regions although the  $\delta^{18}\text{O}$  offset remains at least 4–5‰.

## 6. Discussion

### 6.1. $\delta^{13}\text{C}$ ratite eggshells related to the $\text{CO}_2$ variations

The trend in eggshell  $\delta^{13}\text{C}$  through the Middle Miocene to the latest Miocene or earliest Pliocene to lower values shows an inverse correlation with the evolution of  $p\text{CO}_2$  of Pagani et al. [8,9] (Fig. 2). In their sequence,  $p\text{CO}_2$  remains low, estimated as 200–220 ppmv during the Early Middle Miocene ( $\sim 14$ –16 Ma) and increases to 300–320 ppmv during the Late Miocene ( $\sim 6$  Ma). Assuming a conservative  $\text{C}_3$  dietary ‘endpoint’ of  $\delta^{13}\text{C}_{\text{eggshell}} = -9\text{‰}$  (reflecting  $\delta^{13}\text{C}_{\text{plant}} \sim -25\text{‰}$ ), the data shows that Namibian ratites consumed only  $\text{C}_3$  plants and, by inference,

that these plants dominated Namib floral composition from the Middle to Late Miocene. The 2.5‰ decrease in mean  $\delta^{13}\text{C}$  in ratite eggshells is congruent with an increase in atmospheric  $p\text{CO}_2$  of  $\sim 100$  ppmv over this period, given shifts of  $-0.02\text{‰}/\text{ppmv}$  for  $\text{C}_3$  plants [20]. Another factor can be shifts in  $\delta^{13}\text{C}$  of the atmospheric  $\text{CO}_2$  itself. An organic carbon accumulation event (the Monterey Formation,  $\sim 17$  to 13.5 Ma) manifest in a positive  $\delta^{13}\text{C}$  excursion in marine sediments of about 1–2‰ compared to the Pliocene [33,34], that may have led to a small enrichment in  $^{13}\text{C}$  in the atmospheric  $\text{CO}_2$  at this time. The amplitude of the atmospheric  $\delta^{13}\text{C}_{\text{CO}_2}$ , however, is likely to have remained small ( $<1\text{‰}$ ); hence, the Monterey event, on its own, cannot account for the amplitude of the  $\delta^{13}\text{C}$  trend observed in the ratite eggshells. Other factors are known to influence  $\delta^{13}\text{C}$  in  $\text{C}_3$  plants, but a  $\delta^{13}\text{C}$  decrease of this magnitude would require a marked shift to moister and/or cooler conditions. No clear sedimentological evidence exists for moister conditions in the southern or central/northern Namib over this period [30,35]. Rather all evidence points to continuous aridity from the Middle Miocene to the Pliocene onwards [35].  $\delta^{18}\text{O}$  trends for both regions show small decreases in the latest Miocene biozone, which, as pointed out above, may indicate a slight increase in relative humidity. However, the decrease is statistically significant for the central region only and, moreover, the slight shifts are vastly overshadowed by the large  $\delta^{18}\text{O}$  difference between the two regions in spite of the similarity in  $\delta^{13}\text{C}$ . We conclude that the Namib ratite eggshell  $\delta^{13}\text{C}$  data is consistent with the  $p\text{CO}_2$  trends as proposed by Pagani et al. [8,9] and a small decrease of the  $\delta^{13}\text{C}$  of atmospheric  $\text{CO}_2$ .

The relatively positive mean of  $-8.45\text{‰}$  during the Lower Miocene (18–20 My) is difficult to explain by influence of low  $p\text{CO}_2$  (220–240 ppmv) on  $\text{C}_3$  plants alone. Rather, these data may suggest the presence of a small proportion of obligate CAM, or  $\text{C}_4$ , plants in the ecosystem, or a relative isotopic high value for atmospheric  $\text{CO}_2$  [36]. Previously,  $\delta^{13}\text{C}$  from fossil tooth enamel in Kenya [3] and soil carbonates from North America have hinted at possible earlier, limited presence of  $\text{C}_4$  plants [37] since slightly enriched values were detected in the two proxies.

Our data can provide no direct commentary on a decrease in  $p\text{CO}_2$  in the Pliocene as suggested by boron isotope data [10], because higher mean  $\delta^{13}\text{C}_{\text{eggshell}}$  values show the occurrence of minor but increasing amounts of  $\text{C}_4$  or CAM plants from this time. This is particularly the case for the central Namib. Emergence of a significant difference between the north/central and

southern Pliocene samples sets a trend that continued to the present. However, we have no indication of variability in the intervening periods, where no data exist.

## 6.2. $\delta^{18}\text{O}$ and rainfall regimes

Regions with winter rainfall regimes are characterized by low temperatures and high humidity during the winter, and hot and dry summers. Those that are under the influence of a summer rainfall regime, on the other hand, have low temperatures and low humidity during the winter and warm temperature and higher humidity during the summer. Therefore, the  $^{18}\text{O}$  enrichment offset observed between the central and southern Namib modern and fossil specimens suggests that the two distinct rainfall season patterns (westerlies in the austral winter and tropical systems in the austral summer) have been established since the Miocene. This observation supports inferences about the northern-most extent of the winter rainfall system in southwestern Africa drawn from the distributions of the terrestrial gastropod shells *Trigonephrus* [38]. Today, this gastropod is found only in regions influenced by the winter westerlies rainfall system [39]. These gastropods occur in the southern Namib Miocene and Pliocene aeolianites but never in central Namib aeolianites [38]. The constant values during the Miocene in the southern Namib suggest consistently lower aridity compared to the present. Higher present aridity may in part be related to lower sea level [40], or more likely, to recent (Pliocene and Pleistocene) intensification of the Benguela upwelling system along this coast (see below; e.g. Diester-Haass et al. [44]).

## 6.3. Oceanic and atmospheric interactions

Palaeowind reconstruction based on aeolianite cross-bedding suggests that the Miocene wind regimes were similar to today [41,42]. While the southern Namib aeolianites indicate a prevailing unimodal southerly wind regime from the Middle Miocene, the central Namib aeolianites suggest southern and eastern trade winds [41–43]. These observations indicate the development of near-modern atmospheric circulation conditions for the region from the Middle Miocene.

Data from ODP sites 1085, 1086 and 1087 off the southern Namib coastline show intensification of Benguela upwelling towards the end of the Miocene, denoting the presence of a strong anticyclonic South Atlantic High pressure (SAHP) system off the coast from this time [44]. Since the African plate has moved northwards by  $\sim 5^\circ$  through the Miocene and Pliocene,

upwelling intensification in this region could reflect movement of the continental plate and the sites to positions within the perennial influence of the SAHP, rather than movement of the SAHP itself. The presence of North Atlantic Deepwater [44,45] implies the onset of near-modern Atlantic Ocean circulation at this time.

## 7. Conclusions

Our isotope data for ratite eggshells show that the winter/summer rainfall system dichotomy now characteristic of this region has been established since the formation of the proto-Namib. However, this rainfall zonation does not seem to have brought about distinct plant distributions in the Namib ecosystem until the Pliocene period.  $C_4$  plants are recorded only from around 5 Ma. Although the chronology cannot be specific, the relatively late expansion of  $C_4$  plants into the central Namib at about 22°S is in agreement with the model that proposes earliest occurrence in the equatorial zones and subsequent appearance in the mid-latitudes [4]. Given these observations, we conclude that global, rather than local or regional, events must be advanced to explain the expansion of  $C_4$  grasses into the central Namib region and elsewhere.

If independent lines of evidence contradict the  $pCO_2$  hypothesis for expansion of  $C_4$  plants in the Late Miocene, what plausible alternative explanations exist? Those advanced to date, emphasising the importance of aridity driven in one case by uplift of the Himalayas [1], or in the Great Plains of North America [37], all seem to be insufficiently global in scope to embrace evidence from the Southern Hemisphere — from the Namib where aridity has been continuous since the mid-Miocene and from South America [46]. For the Namib, a marked change in rainfall seasonality may also be ruled out, as we have shown.

Since  $C_4$  plants are adapted to a high radiation growing season [6], we calculated the solar energy budget contrast between summer and winter for latitude 30°S (calculations based on the equations proposed by Laskar et al. [47]). Average insolation contrast between winter and summer is  $271 \pm 95 \text{ W/m}^2$  throughout the last 20 Ma and variability is strongly controlled by precession (98.4% of explained variance). However, no clear trends in seasonal contrast are apparent after the Late Miocene.

Perhaps one remaining explanation for climate changes favouring global  $C_4$  grass expansion is the reorganisation of the Earth's energy budget by means of oceanic and atmospheric circulation. A combination of events that promoted major oceanic and atmospheric

circulation reorganisation occurred towards the end of the Miocene and in the Early Pliocene (Fig. 2). They include Antarctic cryospheric development and increasing isolation, the closure of the Panama seaway [48], with consequent impacts on surface Equator — high latitude temperature gradients and consequently emergence of Arctic glaciation. The observed intensification of the Benguela upwelling system may be one manifestation of this combination of events, the proliferation of  $C_4$  plants in many low and mid-latitude regions of the world may be another.

## Acknowledgements

The authors gratefully acknowledge funding support from the Geological Survey of Namibia, the Namdeb Diamond Corporation (Pty) Ltd., De Beers Africa Exploration, the National Monuments Council of the Republic of Namibia, the French Embassy in Namibia, the Muséum National d'Histoire Naturelle, the University Pierre and Marie Curie of Paris, the CNRS (ECLIPSE), the *Société de Secours des Amis des Sciences*, the National Research Foundation of South Africa, the Palaeoanthropology Scientific Trust and the University of Cape Town. We are grateful to Dr. John Ward for his consistent support of this project and for his helpful comments. We are grateful for the comments of T. Cerling and an anonymous reviewer, which improved the manuscript. This is AEON publication #10.

## Appendix A. Eggshells and biostratigraphy

Eight different types (representing three genera) of struthious eggshells occur in the Namib aeolianite deposits, distinguishable each on the basis of pore complexes and pore density [35]. No two eggshell types are present together in the same stratigraphic level and they are always found in the same stratigraphic superposition. Associated mammal faunas have been used to calibrate the succession. The species are *Namornis oshana* (15–16 My), *Diamantornis corbetti* (14–15 My), *D. spaggiarii* (12–14 My), *D. wardi* (10–12 My), *D. laini* (8–10 My), *Struthio karingarabensis* (5–8 My), *S. daberansensis* (2–5 My) and *S. camelus* (0–2 My). Aepyornithoid eggshells (18–20 My) and *D. spaggiarii* occur in the Sperrgebiet sites.

## Appendix B. Student's *t*-test results

For our statistics treatments, a Levene's test has been applied on all of  $\delta^{13}\text{C}$  and  $\delta^{18}\text{O}$  data between the biostratigraphic zones to control the homogeneity of

variances. This test was significant ( $p < 0.001$  for the carbon,  $p = 0.001$  for the oxygen). Therefore, we did not use the test one-way ANOVA with post-hoc Scheffe's test for multiple comparison (ANOVA assumes that the variances of all groups are equal or near equal) and used a test that does not require this assumption. The Independent Samples  $t$ -test was applied to compare the isotopic fluctuations between each of the biozones in the northern and southern Namib and to the isotopic trends recorded by eggshells:

### B.1. Analytical results in $\delta^{13}\text{C}$ and $\delta^{18}\text{O}$ of southern Namib ratite eggshells

Species	N	Southern Namib			
		$\delta^{13}\text{C}$		$\delta^{18}\text{O}$	
		Mean	S.D.	Mean	S.D.
<i>Struthio camelus</i> (modern)	21	-6.09	1.92	9.55	2.71
<i>Struthio daberensis</i> (2–5 Ma)	19	-9.48	1.46	6.72	2.78
<i>Struthio karingarabensis</i> (5–8 Ma)	4	-11.00	0.58	4.68	1.46
<i>Diamantornis laini</i> (8–10 Ma)	8	-11.03	0.98	6.62	2.16
<i>Diamantornis wardi</i> (10–12 Ma)	42	-10.63	0.94	6.51	3.05
<i>Diamantornis spaggiarii</i> (12–14 Ma)	16	-9.57	1.01	6.80	2.90
<i>Diamantornis corbetti</i> (14–15 Ma)	12	-9.50	0.79	7.33	4.13
<i>Namornis oshanai</i> (15–16 Ma)	10	-8.69	1.01	7.52	1.92
Aepyornithoid (18–20 Ma)	11	-8.45	1.00	5.84	2.22

### B.2. Analytical results in $\delta^{13}\text{C}$ and $\delta^{18}\text{O}$ of central Namib ratite eggshells

Species	N	Central Namib			
		$\delta^{13}\text{C}$		$\delta^{18}\text{O}$	
		Mean	S.D.	Mean	S.D.
<i>Struthio camelus</i> (modern)	11	-3.64	2.41	14.22	2.17
<i>Struthio daberensis</i> (2–5 Ma)	16	-8.20	1.85	11.13	5.36
<i>Struthio karingarabensis</i> (5–8 Ma)	12	-11.63	0.69	9.74	3.27
<i>Diamantornis laini</i> (8–10 Ma)	36	-10.96	1.14	12.10	3.92
<i>Diamantornis wardi</i> (10–12 Ma)	16	-11.07	0.95	15.44	3.26
<i>Diamantornis spaggiarii</i> (12–14 Ma)	–	–	–	–	–
<i>Diamantornis corbetti</i> (14–15 Ma)	19	-9.74	1.05	10.04	4.12
<i>Namornis oshanai</i> (15–16 Ma)	11	-8.23	1.04	12.78	3.98
Aepyornithoid (18–20 Ma)	–	–	–	–	–

### B.3. Comparison between the northern and southern populations for the same eggshell biozone

Species	Comparison southern Namib vs. central Namib					
	$\delta^{13}\text{C}$ $t$ -test for equality of means			$\delta^{18}\text{O}$ $t$ -test for equality of means		
	$t$	df	p	$t$	df	p
<i>Struthio camelus</i> (modern)	3.135	30	0.004	4.923	30	<0.001
<i>Struthio daberensis</i> (2–5 Ma)	2.284	33	0.029	3.121	33	0.004
<i>Struthio karingarabensis</i> (5–8 Ma)	1.627	14	0.126	2.944	14	0.011
<i>Diamantornis laini</i> (8–10 Ma)	0.158	42	0.875	3.797	42	<0.001
<i>Diamantornis wardi</i> (10–12 Ma)	1.605	56	0.114	9.764	56	<0.001
<i>Diamantornis corbetti</i> (14–15 Ma)	0.667	29	0.510	1.779	29	0.086
<i>Namornis oshanai</i> (15–16 Ma)	1.033	19	0.314	3.792	19	0.001

### B.4. $\delta^{13}\text{C}$ trends and $t$ -test results—comparison between each biozone through 20 Ma

Species	$\delta^{13}\text{C}$ trend		
	N	Mean	S.D.
<i>Struthio camelus</i> (modern), central Namib	11	-3.64	2.41
<i>Struthio camelus</i> (modern), southern Namib	21	-6.09	1.92
<i>Struthio daberensis</i> (2–5 Ma), central Namib	16	-8.20	1.85
<i>Struthio daberensis</i> (2–5 Ma), southern Namib	19	-9.48	1.46
<i>Struthio karingarabensis</i> (5–8 Ma)	16	-11.47	0.70
<i>Diamantornis laini</i> (8–10 Ma)	44	-10.98	1.10
<i>Diamantornis wardi</i> (10–12 Ma)	58	-10.75	0.95
<i>Diamantornis spaggiarii</i> (12–14 Ma)	16	-9.56	1.01
<i>Diamantornis corbetti</i> (14–15 Ma)	31	-9.64	0.95
<i>Namornis oshanai</i> (15–16 Ma)	21	-8.45	1.02
Aepyornithoid (18–20 Ma)	11	-8.45	0.99
$t$ -test for equality of means	$t$	df	p
<i>Struthio daberensis</i> (central Namib)– <i>Struthio camelus</i> (central Namib)	5.555	25	<0.001
<i>Struthio daberensis</i> (southern Namib)– <i>Struthio camelus</i> (southern Namib)	6.201	38	<0.001
<i>Struthio karingarabensis</i> – <i>Struthio daberensis</i> (central Namib)	6.614	30	<0.001
<i>Struthio karingarabensis</i> – <i>Struthio daberensis</i> (southern Namib)	4.993	33	<0.001
<i>Diamantornis laini</i> – <i>Struthio karingarabensis</i>	1.675	58	0.099
<i>Diamantornis wardi</i> – <i>Diamantornis laini</i>	1.109	100	0.270



<i>t</i> -test for equality of means	<i>t</i>	df	<i>p</i>
<i>Diamantornis spaggiarii</i> – <i>Diamantornis wardi</i>	4.348	72	<0.001
<i>Diamantornis corbetti</i> – <i>Diamantornis spaggiarii</i>	0.264	45	0.793
<i>Namornis oshanai</i> – <i>Diamantornis corbetti</i>	4.312	50	<0.001
<i>Aepyornithoid</i> – <i>Namornis oshanai</i>	0.019	30	0.985

### B.5. $\delta^{18}\text{O}$ *t*-test results in the southern Namib—comparison between each biozone through 20 Ma

$\delta^{18}\text{O}$ <i>t</i> -test for equality of means	$\delta^{18}\text{O}$ trend—southern Namib		
	<i>t</i>	df	<i>p</i>
<i>Struthio daberasensis</i> – <i>Struthio camelus</i>	3.248	38	0.002
<i>Struthio karingarabensis</i> – <i>Struthio daberasensis</i>	2.744	29	0.010
<i>Diamantornis laini</i> – <i>Struthio karingarabensis</i>	1.603	10	0.140
<i>Diamantornis wardi</i> – <i>Diamantornis laini</i>	0.940	48	0.925
<i>Diamantornis spaggiarii</i> – <i>Diamantornis wardi</i>	0.319	56	0.751
<i>Diamantornis corbetti</i> – <i>Diamantornis spaggiarii</i>	0.407	26	0.687
<i>Namornis oshanai</i> – <i>Diamantornis corbetti</i>	0.131	20	0.897
<i>Aepyornithoid</i> – <i>Namornis oshanai</i>	1.841	19	0.081

### B.6. $\delta^{18}\text{O}$ *t*-test results in the central Namib—comparison between each biozone through 20 Ma

$\delta^{18}\text{O}$ <i>t</i> -test for equality of means	$\delta^{18}\text{O}$ trend—central Namib		
	<i>t</i>	df	<i>p</i>
<i>Struthio daberasensis</i> – <i>Struthio camelus</i>	1.802	25	0.084
<i>Struthio karingarabensis</i> – <i>Struthio camelus</i>	3.831	21	0.001
<i>Struthio karingarabensis</i> – <i>Struthio daberasensis</i>	0.793	26	0.435
<i>Diamantornis laini</i> – <i>Struthio karingarabensis</i>	1.873	46	0.067
<i>Diamantornis wardi</i> – <i>Struthio karingarabensis</i>	4.574	26	<0.001
<i>Diamantornis wardi</i> – <i>Diamantornis laini</i>	2.977	50	0.004
<i>Diamantornis corbetti</i> – <i>Diamantornis wardi</i>	4.234	33	<0.001
<i>Namornis oshanai</i> – <i>Diamantornis corbetti</i>	1.776	28	0.087

## Appendix C. Supplementary data

Supplementary data associated with this article can be found, in the online version, at [doi:10.1016/j.epsl.2005.12.012](https://doi.org/10.1016/j.epsl.2005.12.012).

## References

- [1] J. Quade, T.E. Cerling, J.R. Bowman, Development of Asian monsoon revealed by marked ecological shift during the latest Miocene in northern Pakistan, *Nature* 342 (1989) 163–166.
- [2] T.E. Cerling, Y. Wang, J. Quade, Expansion of  $\text{C}_4$  ecosystems as indicator of global ecological change in the Late Miocene, *Nature* 361 (1993) 344–345.
- [3] M.E. Morgan, J.D. Kingston, B.D. Marino, Carbon isotopic evidence for the emergence of  $\text{C}_4$  plants in the Neogene from Pakistan and Kenya, *Nature* 367 (1994) 162–165.
- [4] T.E. Cerling, J.M. Harris, B.J. MacFadden, M.G. Leakey, J. Quade, V. Eisenmann, J.R. Ehleringer, Global vegetation change through the Miocene–Pliocene boundary, *Nature* 289 (1997) 153–158.
- [5] R.A. Berner, GEOCARB II: a revised model of atmospheric  $\text{CO}_2$  over Phanerozoic time, *Am. J. Sci.* 294 (1994) 56–91.
- [6] J.R. Ehleringer, T.E. Cerling, B.R. Helliker,  $\text{C}_4$  photosynthesis, atmospheric  $\text{CO}_2$ , and climate, *Oecologia* 112 (1997) 285–299.
- [7] EPICA community members, Eight glacial cycles from Antarctic ice core, *Nature* 429 (2004) 623–628.
- [8] M. Pagani, K.T. Freeman, M.A. Arthur, Late Miocene atmospheric  $\text{CO}_2$  concentrations and the expansion of  $\text{C}_4$  grasses, *Science* 285 (1999) 876–879.
- [9] M. Pagani, M.A. Arthur, K.T. Freeman, Miocene evolution of atmospheric carbon dioxide, *Paleoceanography* 14 (1999) 273–292.
- [10] P.N. Pearson, M.R. Palmer, Atmospheric carbon dioxide concentrations over the past 60 million years, *Nature* 406 (2000) 695–699.
- [11] T.A. Franz-Odenaal, J.A. Lee-Thorp, A. Chinsamy, New evidence for the lack of  $\text{C}_4$  grassland expansions during the Early Pliocene at Langebaanweg, South Africa, *Paleobiology* 28 (2002) 378–388.
- [12] A. Zazzo, H. Bocherens, M. Brunet, A. Beauvillain, D. Billiou, H.T. Mackaye, P. Vignaud, A. Mariotti, Herbivore paleodiet and paleoenvironment changes in Chad during the Pliocene using stable isotope ratios of tooth enamel carbonate, *Paleobiology* 26 (2000) 294–309.
- [13] B.J. Johnson, G.H. Miller, P.B. Beaumont, The determination of the Late Quaternary paleoenvironments at Equus Cave, South Africa, using stable isotopes and amino acid racemization in ostrich eggshell, *Palaeogeogr. Palaeoclimatol. Palaeoecol.* 136 (1997) 121–137.
- [14] B.J. Johnson, M.L. Fogel, G.H. Miller, Stable isotopes in modern ostrich eggshell: a calibration for paleoenvironmental applications in semi-arid regions of southern Africa, *Geochim. Cosmochim. Acta* 64 (1998) 2451–2461.
- [15] J.A. Lee-Thorp, A.S. Talma, Stable light isotopes and environments in the southern African Quaternary and Late Pliocene, in: T.C. Partridge, R.R. Maud (Eds.), *The Cenozoic of Southern Africa*, Oxford Monographs on Geology and Geophysics, vol. 40, 2000, pp. 236–251.
- [16] L.A. Stern, G.D. Johnson, C.P. Chamberlain, Carbon isotope signature of environmental change found in fossil ratite eggshells from a South Asian Neogene sequence, *Geology* 22 (1994) 419–422.
- [17] O’Leary, Carbon isotope fractionation in plants, *Phytochemistry* 20 (1981) 553–567.
- [18] G.D. Farquhar, M.H. O’Leary, J.A. Berry, The relation between carbon isotope discrimination and the intercellular carbon dioxide concentration in leaves, *Aust. J. Plant Physiol.* 9 (1982) 121–138.
- [19] G.D. Farquhar, On the nature of the carbon isotope discrimination in  $\text{C}_4$  species, *Aust. J. Plant Physiol.* 10 (1983) 205–226.
- [20] X. Feng, E. Epstein, Carbon isotopes of trees from arid environments and implications for reconstructions atmospheric

- CO<sub>2</sub> concentration, *Geochim. Cosmochim. Acta* 59 (1995) 2599–2608.
- [21] G.D. Farquhar, K.T. Hubick, A.G. Condon, R.A. Richards, Carbon isotope fractionation and plant water-use efficiency, in: P.W. Rundel, J.R. Ehleringer, K.A. Nagy (Eds.), *Stable Isotopes in Ecological Research*, Springer-Verlag, New York, 1989, pp. 21–40.
- [22] W. Dansgaard, Stable isotopes in precipitation, *Tellus* 16 (1964) 435–468.
- [23] H. Föstel, The enrichment of <sup>18</sup>O in leaf water under natural conditions, *Radiat. Environ. Biophys.* 15 (1978) 323–344.
- [24] L.S.L. Sternberg, M.J. DeNiro, H.B. Johnson, Oxygen and hydrogen isotope ratios of water from photosynthetic tissues of CAM and C<sub>3</sub> plants, *Plant Physiol.* 82 (1986) 428–431.
- [25] D. Yakir, Variations in the natural abundances of oxygen 18 and deuterium in plant carbohydrates, *Pl. Cell Environ.* 15 (1992) 1005–1020.
- [26] Y. Von Schirmding, N.J. Van Der Merwe, J.C. Vogel, Influence of diet and age on carbon isotope ratios in ostrich eggshell, *Archaeometry* 24 (1982) 3–20.
- [27] S.J. Milton, W.R.J. Dean, W.R. Siegfried, Food selection by ostrich in southern Africa, *J. Wildl. Manage.* 58 (1994) 234–247.
- [28] V. Barbin, Cathodoluminescence of carbonate shells: biochemical vs diagenetic process, in: M. Page, V. Barbin, P. Blanc, D. Ohnenstetter (Eds.), *Cathodoluminescence in Geosciences*, Springer, Berlin, 2000, pp. 303–329.
- [29] V. Barbin, K. Ramseier, J.P. Debenay, E. Schein, M. Roux, D. Decrouez, Cathodoluminescence of recent biogenic carbonates: an environmental and ontogenic fingerprint, *Geol. Mag.* 128 (1991) 19–26.
- [30] L. Ségalen, Evolution environnementale du Désert du Namib depuis le Miocène. Apports de la sédimentologie et des rapports isotopiques (<sup>13</sup>C, <sup>18</sup>O) mesurés sur des coquilles de ratites. PhD thesis, Univ. Pierre and Marie Curie, Paris (2003) (275 pp.).
- [31] H.G. Machel, R.A. Mason, A.N. Mariano, A. Mucci, Causes and emission of luminescence in calcite and dolomite, in: C.E. Barker, O.C. Kopp (Eds.), *Luminescence Microscopy: Quantitative and Qualitative Aspects*, SEMP, 1991, pp. 9–25.
- [32] L. Ségalen, M. Renard, M. Pickford, B. Senut, I. Cojan, L. Le Callonnec, P. Rognon, Environmental and climatic evolution of the Namib Desert since the Middle Miocene: the contribution of carbon isotope ratios in ratite eggshells, *C. R. Géosci.* 334 (2002) 917–924.
- [33] J. Zachos, M. Pagani, L. Sloan, E. Thomas, K. Billups, Trends, rhythms, and aberrations in global climate 65 Ma to present, *Science* 292 (2001) 686–693.
- [34] M. Mutti, A.W. Droxler, A.D. Cunningham, Evolution of the northern Nicaragua rise during the Oligocene–Miocene: drowning by environmental factors, *Sediment. Geol.* 175 (2005) 237–258.
- [35] M. Pickford, B. Senut, Geology and palaeobiology of the Namib Desert, southwestern Africa, *Commun. Geol. Surv. Namib., Windhoek, Mem.* 18 (1999) (155 pp.).
- [36] B.H. Passey, T.E. Cerling, M.E. Perkins, M.R. Voorhies, J.M. Harris, S.T. Tucker, Environmental change in the great plains: an isotopic record from fossil horses, *J. Geol.* 110 (2002) 123–140.
- [37] D.L. Fox, P.L. Koch, Tertiary history of C<sub>4</sub> biomass in the Great Plains, USA, *Geology* 31 (1994) 809–812.
- [38] J. Ward, I. Corbett, M. Pickford, B. Senut, Terrestrial gastropods in the southern Namib: evidence for winter rainfall in the Miocene? SASQUA Abstr. (1993) 24.
- [39] A.C. Van Bruggen, Studies on the Land Molluscs of Zululand with notes on the distribution of land molluscs in southern Africa, *Zoöl. Verh.* 103 (1969) 3–116.
- [40] B.U. Haq, J. Hardenbol, P.R. Vail, Chronology of fluctuating sea-levels since the Triassic, *Science* 234 (1987) 1156–1167.
- [41] J. Ward, Eolian, fluvial and pan (playa) facies of the Tertiary Tsondab Sandstone Formation in the Central Namib Desert, Namibia, *Sediment. Geol.* 55 (1988) 143–162.
- [42] L. Ségalen, P. Rognon, M. Pickford, B. Senut, L. Emmanuel, M. Renard, J. Ward, Reconstitution des morphologies dunaires et du régime des paléovents dans le Proto-Namib au cours du Miocène, *Bull. Soc. Géol. Fr.* 175 (2004) 537–546.
- [43] G. Kokurek, N. Lancaster, M. Carr, A. Frank, Tertiary Tsondab Sandstone Formation: preliminary bedform reconstruction and comparison to modern Namib Sand Sea dunes, *J. Afr. Earth Sci.* 29 (1999) 629–642.
- [44] L. Diester-Haass, P.A. Meyers, T. Bickert, Carbonate crash and biogenic bloom in the Late Miocene: evidence from ODP Sites 1085, 1086, and 1087 in the Cape Basin, southeast Atlantic Ocean, *Paleoceanography* 19 (2004) PA1007, doi:10.1029/2003PA 000933.
- [45] B.P. Flower, J.P. Kennett, The Middle Miocene climate transition: East Antarctic ice sheet development, deep ocean circulation and global carbon cycling, *Palaeogeogr. Palaeoclimatol. Palaeoecol.* 108 (1994) 537–555.
- [46] C. Latorre, J. Quade, W.C. McIntosh, The expansion of C<sub>4</sub> grasses and global climate change in the Late Miocene: stable isotope evidence from the Americas, *Earth Planet. Sci. Lett.* 146 (1997) 83–96.
- [47] J. Laskar, F. Joutel, F. Boudin, Orbital, precessional, and insolation quantities for the Earth from –20 Myr to +10 Myr, *Astron. Astrophys.* 270 (1993) 522–533.
- [48] K.W. Burton, H.F. Ling, R.K. O’Nions, Closure of the Central American Isthmus and its effect on deep-water formation in the North Atlantic, *Nature* 386 (1997) 382–385.